

pubs.acs.org/JACS Article

# Using Photoexcited Core/Shell Quantum Dots To Spin Polarize Appended Radical Qubits

Jacob H. Olshansky,<sup>‡</sup> Samantha M. Harvey,<sup>‡</sup> Makenna L. Pennel, Matthew D. Krzyaniak, Richard D. Schaller, and Michael R. Wasielewski\*



Cite This: J. Am. Chem. Soc. 2020, 142, 13590-13597



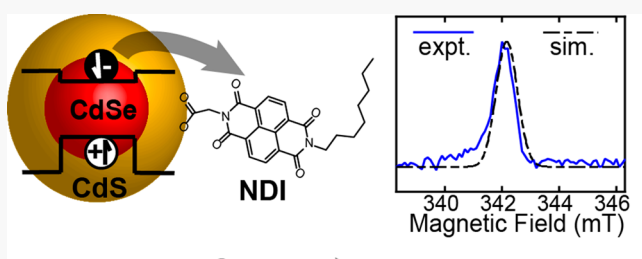
**ACCESS** 

Metrics & More

Article Recommendations

s Supporting Information

ABSTRACT: The synthetic tunability, flexibility, and rich spin physics of semiconductor quantum dots (QDs) make them promising candidates for quantum information science applications. However, the rapid spin relaxation observed in colloidal quantum dots limits their functionality. In the current work, we demonstrate a method to harness photoexcited spin states in QDs to produce long-lived spin polarization on an appended organic ligand molecule. We present a system composed of CdSe/CdS core/shell QDs, covalently linked to naphthalenediimide (NDI) electron-accepting molecules. The electron transfer dynamics from photoexcited QDs to the appended NDI ligands is explored as a



photoexcited QD spin polarized NDI

function of both shell thickness and number of NDIs per QD. Transient EPR spectroscopy shows that the photoexcited QDs strongly spin polarize the NDI radical anion, which is interpreted in the context of both the radical pair and the triplet mechanisms of spin polarization. This work serves as an initial step toward using photoexcited QDs to strongly spin polarize organic radicals having long spin relaxation times to serve as spin qubits in quantum information science applications.

### **■ INTRODUCTION**

The promise that quantum information science (QIS) holds to revolutionize computation, communication, and sensing is accelerating research in this field. 1,2 However, the exact materials that will comprise these emergent technologies remain an open question. 2,3 A particularly prominent class of materials, semiconductor quantum dots (QDs), has been proposed for quantum computation and communication applications. 4-9 QDs grown by molecular beam epitaxy in all-solid-state devices are the most widely studied form for these applications, but colloidal QDs are also attractive candidates owing to the tunability of their size, 10 shape, 11 and composition. 12 Optical excitation in colloidal QDs is particularly intriguing because it offers a way to selectively address specific QDs (i.e., by size or composition) and can generate well-defined spin states, 13,14 thus satisfying two key criteria of functioning qubits. 15

The spin dynamics of photoexcited charges in the archetypal cadmium chalcogenide (CdE) colloidal QDs have been probed by a variety of optical and magneto-optical techniques, including time-resolved Faraday rotation, <sup>6,7,13,16</sup> degree of emissive circular polarization, <sup>17</sup> polarized pump—probe spectroscopy, <sup>18</sup> and cross-polarized transient grating spectroscopy. <sup>14,19</sup> From this a generalized picture of spin dynamics in these colloidal QDs has been developed. Due to extensive spin—orbit coupling, the spin states in CdE QDs are best described by their total angular momentum. The two lowest

energy states have total angular momenta of F=1 and F=2 and are termed "bright" and "dark" excitonic states, respectively. The F=2 dark state lies approximately  $\Delta E_{\rm BD}=2-20$  meV below the bright state. Spin relaxation between these two states is suggested to occur on the subpicosecond to tens of picoseconds time scale as a result of hole spin flips, resulting in rapidly equilibrated Boltzmann populations. A slow component to spin relaxation is also observed (hundreds of picoseconds to a few nanoseconds) and is ascribed to both intralevel relaxation (e.g.,  $+2 \rightarrow -2$  within the dark state) and electron spin flips.  $^{6,14,17,18}$  In either case, photogenerated spin coherence in these systems does not live long enough to support the microwave-based spin manipulations required for quantum logic gates (>100 ns). A strategy to harness these spin states prior to relaxation is therefore necessary.

Organic molecules offer a promising platform for supporting long-lived spin coherences owing to their weak spin—orbit coupling.<sup>23</sup> Therefore, transferring spin coherence, or at least spin polarization, from a photoexcited QD to an organic

Received: June 4, 2020 Published: July 10, 2020





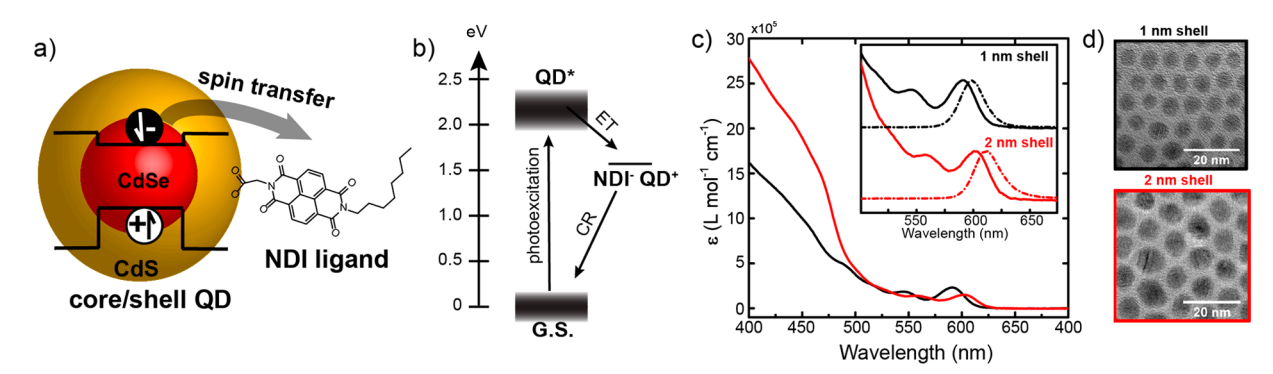


Figure 1. Schematic of the donor–acceptor system. (a) Diagram of the CdSe/CdS core/shell QD and the NDI ligand that acts as the electron acceptor. (b) Energy diagram of electron transfer (ET) to create the NDI<sup>-•</sup>–QD<sup>+</sup> species and charge recombination (CR) to the ground state. (c) UV–vis absorption (solid lines) and photoluminescence (dashed lines) of 1 nm shell (black) and 2 nm shell (red) QDs. (d) Transmission electron microscopy images of QDs.

molecule is of keen interest. With this aim in mind, it is worth briefly reviewing efforts to understand and control spin in QD—molecular conjugate systems. Coherent spin transfer has been demonstrated from photoexcited QDs of one size to molecularly linked QDs of another size. Spin-selective charge extraction from QDs has also been demonstrated when functionalized with chiral molecules via the chiral-induced spin selectivity (CISS) effect. Photoexcited QDs have been used to efficiently sensitize molecular triplet states via triplet energy transfer. Sensitize molecular triplet states via triplet energy transfer. Turthermore, spin state control in photoexcited QD—organic molecule conjugates has been shown in the context of the spin-correlated radical pair (SCRP) model.

In both triplet energy transfer studies and the SCRP work, longer-lived QD excited states display primarily triplet character. The SCRP studies are of interest in the context of the research presented here. In two of these studies, photoexcitation of an organic chromophore and subsequent electron transfer to a QD results in a radical pair state (QD-molecule<sup>+</sup>) that undergoes radical pair intersystem crossing followed by charge recombination to yield a molecular triplet state. 32,33 This process is further verified by transient electron paramagnetic resonance (EPR) measurements.<sup>33</sup> In a third study, spin control is demonstrated by selectively exciting either the organic molecule or the OD.<sup>34</sup> When the molecule is excited, rapid charge separation and recombination outcompetes spin interconversion, allowing for return to the singlet ground state. When the QD is excited, however, the QD--molecule+ state recombines to a molecular triplet state.<sup>34</sup> These studies demonstrate the possibilities for spin control in photogenerated QD-molecular systems. However, they have been limited to QD--molecule+ radical pairs and furthermore do not directly probe the charge-separated state.

In the work presented here, we directly probe via transient EPR spectroscopy a QD<sup>+</sup>-molecule<sup>-</sup> state that is generated by QD photoexcitation. These measurements are enabled using core/shell CdSe/CdS QDs that can support long-lived charge-separated states. We first investigate the dynamics of photoexcited electron transfer from CdSe/CdS core/shell QDs to a naphthalenediimide (NDI) electron acceptor as a function of both CdS shell thickness and NDI surface coverage. This serves as a means both to more confidently determine the charge transfer rates relevant for the EPR measurements but also to benchmark shell thickness-dependent electron transfer in the less explored CdSe/CdS core/shell system (compared to CdSe/ZnS). A polarized spin state

assigned to the NDI radical anion is observed in the transient EPR data. The signal is nearly entirely absorptive, suggestive of a polarization mechanism analogous to the triplet mechanism (TM) in which polarized spins are generated by charge separation from a photogenerated spin-polarized triplet state. So In this case, the photoexcited QD serves as the "triplet". Temperature-dependent EPR measurements suggest that this polarization may arise from the population difference in the dark and bright states of the QD. Using photoexcited QDs to spin polarize surface-bound molecular qubits is an important step toward harnessing the rich spin physics and synthetic tunability of colloidal QDs for QIS applications.

#### ■ RESULTS AND DISCUSSION

The system explored in this paper is shown in Figure 1. CdSe/ CdS core/shell QDs serve as both the light absorber and the electron donor. A modified NDI ligand with a carboxylate functional group linker serves as the electron acceptor (NDI absorbs blue of 400 nm, avoiding coexcitation, see Supporting Information (SI)). Approximate energetics for the system are shown in Figure 1b. Prior electrochemical measurements have shown that the approximate valence band energy of similar CdSe/CdS core/shell QDs is 1.2 V vs SCE. 40 However, it should be noted that electrochemical measurements on QD band energies are subject to large errors (hundreds of meVs), and therefore, we represent these states as a distribution. Since the reduction potential of NDI is -0.48 V vs  $SCE^{42}$  and the QD excited state energy is 2.1 eV, the approximate free energy change for charge separation is -0.4 eV. The optical absorption and emission of the QDs are shown in Figure 1c. Both core/shell samples are grown from the same batch of 3.3 nm CdSe core QDs following previously published synthetic procedures. 40,43 The 2 nm shell sample exhibits red-shifted emission and absorption due to carrier delocalization and also shows enhanced absorption in the 400-450 nm range as a result of increased CdS volume. The photoluminescence quantum yields were 13% and 68% for the 1 and 2 nm shell samples, respectively. Transmission electron microscopy images are shown in Figure 1d and were used to calculate average diameters of 5.6 and 7.7 nm. See SI for sizing histograms.

The QD-NDI conjugates were prepared with a range of NDI equivalents per QD by adding progressively more NDI ligand to a dilute QD solution in toluene (see SI for details). The carboxylate group serves as the binding head to the QD

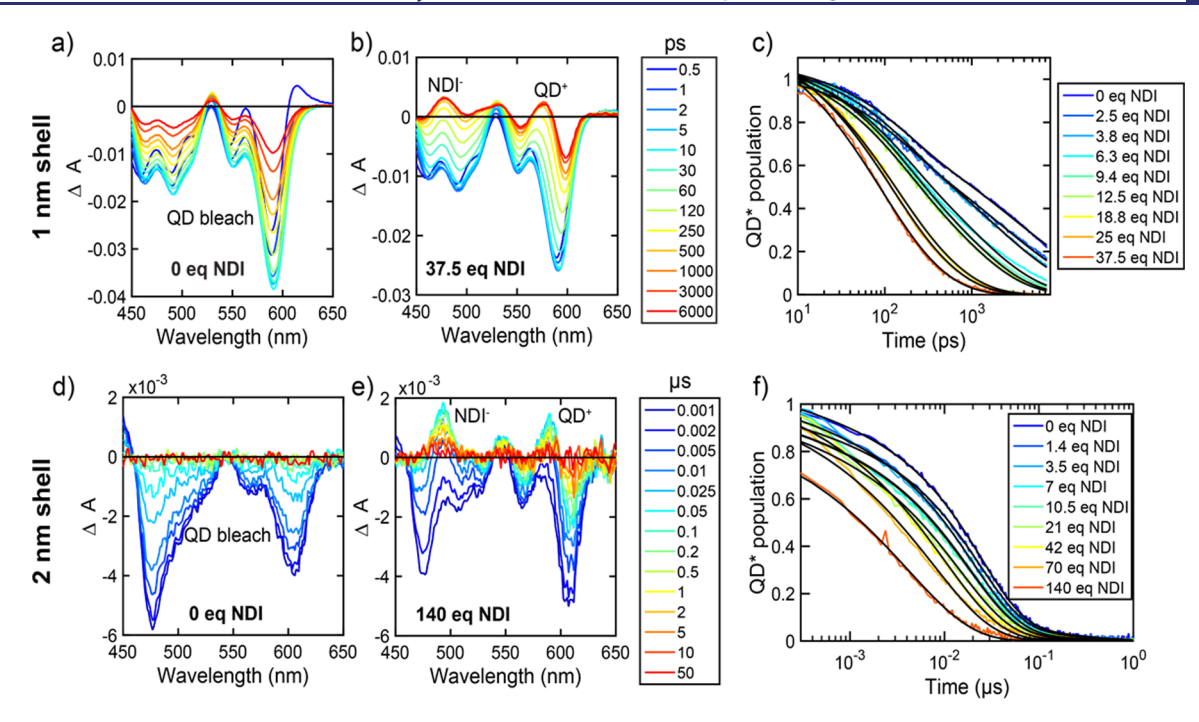


Figure 2. Ultrafast transient spectra and population dynamics in the 1 nm shell (a-c) and 2 nm shell (d-f) QD-NDI systems. (a and d) Transient spectra of the QDs with no NDI added, illustrating the QD bleach recovery. (b and e) Transient spectra of the QD-NDI conjugates illustrating evolution from the QD bleach at early times to an NDI $^{-\bullet}$ -QD $^{+}$  state at longer times. (c and f) Relative population of the QD\* state (based on basis spectra deconvolution into a QD bleach and NDI $^{-\bullet}$ -QD $^{+}$  components). Increasing equivalents of NDI per QD result in a faster decay of the QD\* population.

surface. The as-synthesized CdSe/CdS core/shell QDs are primarily coated with oleic acid, which can be ligand exchanged for other carboxylic acid ligands (such as our NDI ligand). We believe all NDI added binds because (1) the NDI ligand is only sparingly soluble in toluene but produces a scatter-free solution when combined with QDs and (2) the free NDI does not appear in solution NMR spectra when mixed with the QDs. In addition, we found that the NDI ligand did not bind to the native CdSe QDs, which were functionalized with phosphonic acid ligands. This is consistent with previous work and was remedied by heating the CdSe QD samples in oleic acid for a day prior to treatment with NDI (see SI for details).

Prior to analyzing the spin characteristics in this QDmolecular dyad, we first aimed to obtain a full picture of the charge transfer dynamics. Such information aids in our interpretation of the spin dynamics as well as provides benchmark rates for shell-dependent electron transfer from CdSe/CdS core/shell QDs. To probe these charge transfer dynamics, we turned to transient absorption spectroscopy. Transient absorption data were collected for the CdSe core, 1 nm shell CdSe/CdS, and 2 nm shell CdSe/CdS QDs with a range of NDI equivalents per QD. Example transient spectra are shown in Figure 2, highlighting the core/shell QDs with either no NDI or many NDI ligands (see SI for all transient spectra). The slower dynamics of the 2 nm shell sample precluded the collection of meaningful data on the femtosecond to picosecond time scale. In the absence of NDI, all samples exhibit a multiexponential QD bleach recovery corresponding to all radiative and nonradiative recombination pathways native to the QDs (Figure 2a and 2d). Upon addition of NDI, we observe new spectral features associated with both NDI-• and QD+, confirming the presence of photoinitiated charge separation. NDI- most notably has a prominent

absorption feature at ~480 nm,<sup>42</sup> which is observed in all transient spectra that include NDI. The derivative-like feature near the QD band edge is assigned to a Stark-shifted QD absorption resulting from the electric field between the separated charges and has been described previously in similar systems.<sup>45,46</sup> Importantly, both NDI<sup>-•</sup> and QD<sup>+</sup> features appear in the same ratio regardless of the number of NDI equivalents and decay in concert. This suggests that we are generating a one-to-one NDI<sup>-•</sup> and QD<sup>+</sup> pair that annihilates via charge recombination.

To quantify charge separation rates, we deconvolved all transient spectra into a QD bleach (i.e., a QD excited state, QD\*) basis spectrum and an NDI-•-QD+ basis spectrum. From these basis spectra, we could construct time-resolved population traces for the QD\* and NDI-•-QD+ states. The QD\* populations for the core/shell samples are shown in Figure 2c and 2f. All other basis spectra and population traces are shown in the SI. Population transients were fit to multiexponential functions, as described in the SI, to yield two independent estimates for the charge separation rate constant. These two independent estimates come from either fitting the decay of the QD\* state or fitting the rise of the NDI -- QD+ state. By plotting these rate constants as a function of NDI equivalents per QD (Figure 3a and 3b), one can extract a bimolecular electron transfer rate constant  $(k_{cs})$  in accordance with the relation  $k_{cs,tot} = Nk_{cs}$ , where N is the number of acceptors per QD. The linearity of these plots further validates our method and assumption that each NDI ligand added does indeed bind to the surface in the range studied. The bimolecular rate constants (utilizing either QD\* or  $\mathrm{NDI}^{-\bullet}\mathrm{-QD}^{\scriptscriptstyle+}$  populations) are plotted as a function of shell thickness in Figure 3c. Although both populations yield similar charge transfer rate constants, the rate constant from the QD\* population is consistently smaller than that derived from the

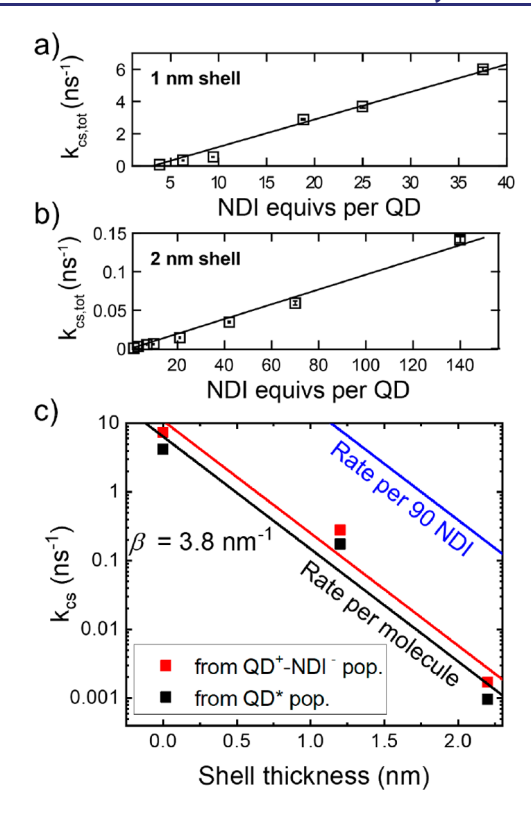


Figure 3. Extracting bimolecular charge separation rates for QD–NDI conjugates. (a and b) Charge separation rate constants as a function of NDI equivalents per QD, extracted from the QD\* population. Slope of the linear fits gives a bimolecular rate constant per NDI ligand. (c) Bimolecular rate constants as a function of shell thickness using the QD\* population (black) and NDI-•-QD+ population (red) to extract rates. Also shown are the expected rate constants with 90 NDI per QD, the approximate concentration used for EPR experiments.

NDI<sup>-•</sup>–QD<sup>+</sup> populations. This is likely a result of using a stretched exponential for the QD\* fits and an intensity-weighted average of two exponentials in the NDI<sup>-•</sup>–QD<sup>+</sup> fits (see SI). It should be noted that stretched exponentials have been demonstrated as an adequate and physically meaningful way to fit QD PL quenching by molecular charge acceptors.<sup>47</sup>

With the bimolecular rate constants determined, we can now analyze the shell thickness dependence of these values. The rate constants can be fit to an exponential decay  $(k_{cs} \propto e^{-\beta d})$  with a tunneling coefficient of  $\beta=3.8~{\rm nm}^{-1}$ . This value is comparable to  $\beta=3.5~{\rm nm}^{-1}$  determined for electron transfer from CdSe/ZnS core/shell QDs <sup>48</sup> as well as  $\beta=3.3~{\rm nm}^{-1}$  from CdSe/CdS core/shell QDs. <sup>49</sup> However, there exist conflicting reports on this value, with a third study using CdSe/CdS core/shell QDs reporting  $\beta=1.3~{\rm nm}^{-1}$ . Effective mass-based approximations have also predicted tunneling coefficients for CdSe/CdS electron transfer of  $\beta=1.8~{\rm and}~2.2~{\rm nm}^{-1}$ . The variety of reported values likely arises from conflicting methods for determining the rates, preparing the QDs, and assessing the number of molecular acceptors.

For the purposes of the current study, determining the shell-thickness-dependent bimolecular charge transfer rate constant serves as a first step toward predicting the relevant rates in the EPR experiments presented below. We can use it to estimate the rate constant with ~90 NDI ligands bound per QD (blue line), which is the approximate concentration used in the EPR experiments. From this analysis, we expect electron transfer to

occur in about  $\sim$ 100 ps for the 1 nm shell and  $\sim$ 5 ns for the 2 nm shell, values close to or slower than spin relaxation in the QD. In addition, it should be noted that the transient absorption experiments were all done at room temperature, while the EPR experiments are performed between 5 and 80 K. In the absence of trap-mediated charge transfer, which would enhance observed charge transfer rates, photoexcited charge transfer from CdSe/CdS core/shell QDs has been shown to be relatively temperature independent. 52 Therefore, the rate constants indicated by the blue line in Figure 3c serve as an upper bound and likely a reasonable estimate of the rate constants that will be present in the EPR experiments. To ensure that the charge-separated states live long enough for EPR measurements, recombination rate constants were analyzed by fitting NDI-•-QD+ populations to stretched exponentials. The core/shell samples had recombination time constants on the order of a few microseconds, while the core sample was closer to ~20 ns (see SI). The more rapid recombination seen in the core-only samples, precludes their utility for conducting EPR-based spin manipulations.

With the charge dynamics established for the NDI-QD conjugates, we turn to time-resolved EPR to understand their spin dynamics. At the outset, there is scant evidence that a measurement technique as slow as EPR (~10 ns) can detect spin states in cadmium chalcogenide QDs because the numerous heavy cadmium atoms lead to rapid spin relaxation, as mentioned in the Introduction. In fact, our own attempts to measure conduction-band electrons photogenerated in CdSe QDs (following work from the Gamelin group<sup>53</sup>) by continuous-wave (CW) EPR yielded no signal, even at 5 K. This contrasts with first-row transition metal oxide nanoparticles such as ZnO and TiO2. The Gamelin group has shown size-dependent CW EPR signals from electrons in ZnO QDs,54 and the radical pair model has been used to describe transient EPR spectra of photogenerated species on TiO<sub>2</sub> nanoparticles. 55,56 In the present study, despite the lack of a direct EPR signal from any charges within the CdSe QD, we demonstrate that QD photoexcitation and subsequent electron transfer generates a spin-polarized NDI\*-.

In the transient EPR experiments, we observe a polarized and mostly absorptive signal associated with the NDI<sup>•–</sup> (Figure 4). The signal intensity is temperature dependent and can be fit to an absorptive peak centered at the NDI<sup>•–</sup> gvalue of 2.003 (see SI for calculations). While it is difficult to quantify the degree of spin polarization (see below), both QD samples (1 nm shells and 2 nm shells) showed similar signal-to-noise ratios employing similar experimental acquisition times and sample concentrations, which means that the signal intensities agree to within about an order of magnitude.

We propose that this absorptive signal results from the TM of spin polarization.  $^{35,36}$  In this case, the photoexcited QD serves as the triplet, consistent with numerous studies that observe significant triplet character of this state.  $^{31,33,34}$  At the lowest temperatures there is evidence of a small emissive EPR feature in the signal (Figure 4b). This spectrum was simulated by including a small contribution from an absorptive/emissive (A/E) response, which is common to triplet-generated, SCRP.  $^{39,57}$  Employing a combination of the SCRP mechanism and the TM to model transient EPR spectra of charge-separated states has precedent in studies on hole transfer from photoexcited  $C_{60}$  to either tetramethylbenzidine  $^{58}$  or a zinc porphyrin.  $^{39}$  In both of these studies, transient spectra were fit to a superposition of absorptive signals ascribed to the TM and

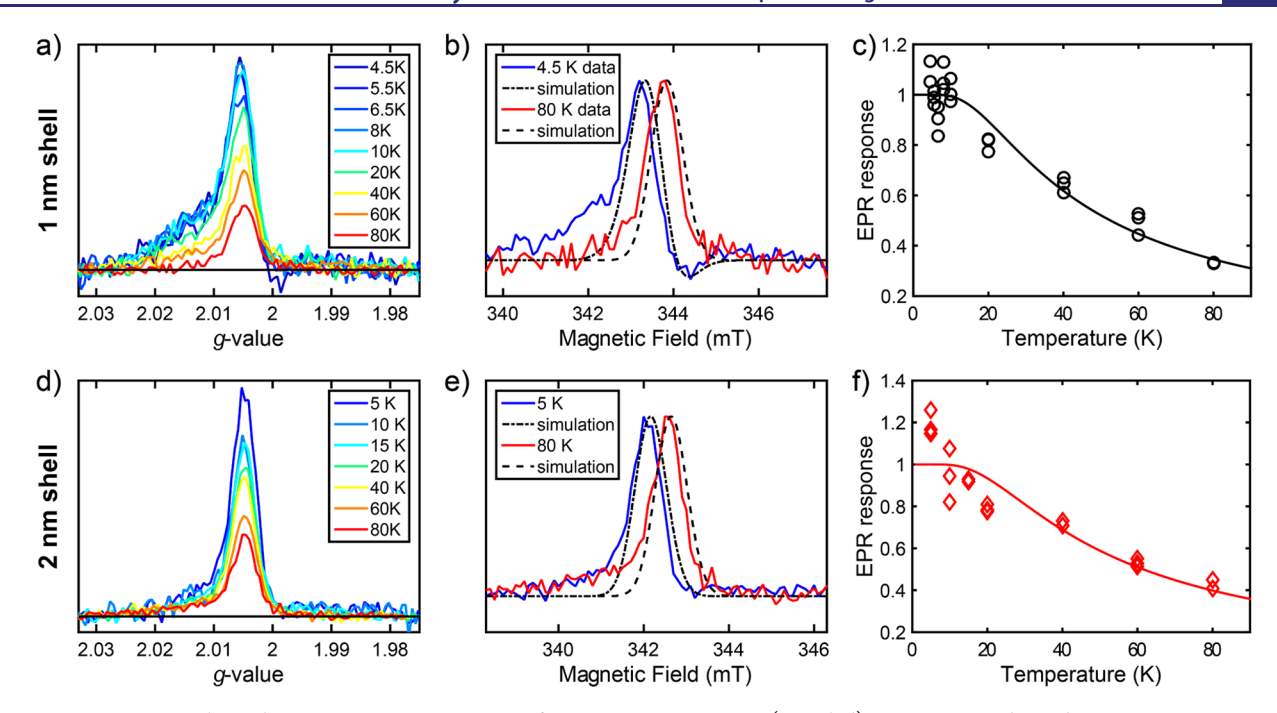


Figure 4. Temperature-dependent transient EPR spectra of QD-NDI conjugates. (a and d) Temperature-dependent transient EPR spectra recorded 100 ns after a 550 nm (7 ns, 2 mJ) laser pulse. Data are shown vs g-value since the resonant frequency was temperature dependent. (b and e) Data for the lowest and highest temperature data overlain with simulations derived from the NDI anion. Again, data are shifted due to temperature-dependent frequency shifts. (c and f) Maximum EPR response 100 ns after laser flash in each of three scans collected at each temperature. Data are fit to eq 1.

E/A or A/E signals resulting from a SCRP. This precedent bolsters our interpretation, but the precise spin states in the QD that are responsible for spin polarizing NDI<sup>•–</sup> remain an open question.

Since the degree of polarization reflects the population difference between the spin sublevels and the observed spin polarization is most likely being generated by the TM, the inability to observe the QD "triplet" directly makes it difficult to quantify the observed spin polarization. In contrast, in a singlet-born radical pair, the  $T_{+1}$  and  $T_{-1}$  states are not populated initially; thus, the polarization of the  $S-T_0$  mixed states relative to either the  $T_{+1}$  or  $T_{-1}$  state is 100%. Given the relative insensitivity of transient EPR using a CW microwave source with no field modulation, the excellent signal-to-noise that we observed suggests very high polarization.

To better understand the origins of spin polarization from the QD, it is worth revisiting the relevant spin relaxation times. Equilibration between the dark and the bright states occurs in a few picoseconds, well before electron transfer occurs in our case. The slower spin relaxation component, associated with intralevel relaxation, occurs on the order of a few nanoseconds. This is slower than electron transfer from the 1 nm shell ( $\sim$ 100 ps) but outcompetes electron transfer from the 2 nm shell (~5 ns). The similarity of EPR signals in the 1 and 2 nm shell samples, however, suggests that this relaxation process is not important for the observed spin polarization; if it was important, the 1 and 2 nm samples should be quite distinct. This begs the question: can spin polarization of NDI\*- occur on a slower time scale than spin relaxation in the QD? We believe that this would be possible if the thermally equilibrated bright and dark exciton states (total angular momenta of F = 1and 2, respectively) populate spin sublevels in the chargeseparated state with different efficiencies. In this scenario, the observed polarization would be proportional to the population

difference between the bright and the dark state, expressed by the following equation

where  $P_{F=1}$  and  $P_{F=2}$  are the bright and dark state Boltzmann populations, respectively, which have an energy difference of  $\Delta E_{\rm BD}$ . The temperature-dependent EPR signal is fit to this functional form (Figure 4c and 4f) and yields values of  $\Delta E_{\rm BD} = 5.1$  and 5.7 meV for the 1 and 2 nm shells, respectively. These values are well within the range of reported  $\Delta E_{\rm BD}$ , and their similarity is not unsurprising for their geometries, which are predicted to produce similar electron—hole overlap integrals. This analysis offers one possible explanation for the origin of spin polarization in our QD—molecular system and a first step toward understanding this interesting phenomenon.

## CONCLUSIONS

In conclusion, we have designed a QD—molecular system that can generate long-lived spin polarization on the molecular acceptor following photoexcitation of the QD. We first establish an understanding of the photoexcited electron transfer dynamics by varying the shell thickness of CdSe/CdS core/shell QDs and the number of NDI electron acceptors per QD. We then use transient EPR to show that this electron transfer process also conveys spin polarization from the QD to the NDI. The spin polarization on the NDI survives for >100 ns, which is significantly longer than the rapid (few nanoseconds) spin relaxation inherent to colloidal QDs. These experiments represent a promising route toward generating long-lived and well-defined spin qubit states. Specifically, the highly absorbing and tunable QD entity can

be used to photogenerate a highly spin-polarized state, and the rapid spin relaxation inherent to QDs can be avoided by transferring this polarization onto an organic molecule.

#### ASSOCIATED CONTENT

## **Solution** Supporting Information

The Supporting Information is available free of charge at https://pubs.acs.org/doi/10.1021/jacs.0c06073.

Experimental details, including instrumental techniques, QD synthesis, transmission electron microscopy, additional transient optical absorption data and transient EPR data, and kinetic analysis (PDF)

## AUTHOR INFORMATION

#### **Corresponding Author**

Michael R. Wasielewski — Department of Chemistry and Institute for Sustainability and Energy at Northwestern, Northwestern University, Evanston, Illinois 60208-3113, United States; orcid.org/0000-0003-2920-5440; Email: m-wasielewski@northwestern.edu

#### **Authors**

Jacob H. Olshansky — Department of Chemistry and Institute for Sustainability and Energy at Northwestern, Northwestern University, Evanston, Illinois 60208-3113, United States;

orcid.org/0000-0003-3658-1487

Samantha M. Harvey – Department of Chemistry and Institute for Sustainability and Energy at Northwestern, Northwestern University, Evanston, Illinois 60208-3113, United States

Makenna L. Pennel – Department of Chemistry and Institute for Sustainability and Energy at Northwestern, Northwestern University, Evanston, Illinois 60208-3113, United States

Matthew D. Krzyaniak — Department of Chemistry and Institute for Sustainability and Energy at Northwestern, Northwestern University, Evanston, Illinois 60208-3113, United States; orcid.org/0000-0002-8761-7323

Richard D. Schaller – Department of Chemistry and Institute for Sustainability and Energy at Northwestern, Northwestern University, Evanston, Illinois 60208-3113, United States; Center for Nanoscale Materials, Argonne National Laboratory, Lemont, Illinois 60439, United States

Complete contact information is available at: https://pubs.acs.org/10.1021/jacs.0c06073

#### **Author Contributions**

<sup>‡</sup>J.H.O. and S.M.H.: These authors contributed equally. **Notes** 

The authors declare no competing financial interest.

## ■ ACKNOWLEDGMENTS

This work was supported by the Department of Energy, Office of Science, Office of Basic Energy Sciences Award DE-SC0020168 (M.R.W.) S.M.H was supported by the National Science Foundation Graduate Research Fellowship Program under Grant No. DGE-1324585. M.P. would like to acknowledge the International Institute of Nanotechnology summer undergraduate research experience. This material is based upon work supported by the National Science Foundation (NSF) under Grant Number EEC-1757618. Any opinions, findings, and conclusions or recommendations expressed in this material are those of the authors and do not necessarily reflect the views of the NSF. This work was performed, in part,

at the Center for Nanoscale Materials, a U.S. Department of Energy Office of Science User Facility, and supported by the U.S. Department of Energy, Office of Science, under Contract No. DE-AC02-06CH11357. This work also made use of the EPIC facility of Northwestern University's NUANCE Center, which has received support from the Soft and Hybrid Nanotechnology Experimental (SHyNE) Resource (NSF ECCS-1542205), the MRSEC program (NSF DMR-1720139) at the Materials Research Center, the International Institute for Nanotechnology (IIN), the Keck Foundation, and the State of Illinois, through the IIN.

#### REFERENCES

- (1) Degen, C. L.; Reinhard, F.; Cappellaro, P. Quantum sensing. Rev. Mod. Phys. 2017, 89, 035002.
- (2) Ladd, T. D.; Jelezko, F.; Laflamme, R.; Nakamura, Y.; Monroe, C.; O'Brien, J. L. Quantum computers. *Nature* **2010**, 464, 45–53.
- (3) Popkin, G. Quest for qubits. Science 2016, 354, 1090-1093.
- (4) Burkard, G.; Engel, H.-A.; Loss, D. Spintronics and quantum dots for quantum computing and quantum communication. *Fortschr. Phys.* **2000**, *48*, 965–986.
- (5) Loss, D.; DiVincenzo, D. P. Quantum computation with quantum dots. *Phys. Rev. A: At., Mol., Opt. Phys.* **1998**, *57*, 120–126.
- (6) Gupta, J. A.; Awschalom, D. D.; Peng, X.; Alivisatos, A. P. Spin coherence in semiconductor quantum dots. *Phys. Rev. B: Condens. Matter Mater. Phys.* **1999**, 59, R10421–R10424.
- (7) Ouyang, M.; Awschalom, D. D. Coherent spin transfer between molecularly bridged quantum dots. *Science* **2003**, *301*, 1074–1078.
- (8) Kloeffel, C.; Loss, D. Prospects for spin-based quantum computing in quantum dots. *Annu. Rev. Condens. Matter Phys.* **2013**, 4, 51–81.
- (9) Awschalom, D. D.; Bassett, L. C.; Dzurak, A. S.; Hu, E. L.; Petta, J. R. Quantum spintronics: Engineering and manipulating atom-like spins in semiconductors. *Science* **2013**, 339, 1174–1179.
- (10) Murray, C. B.; Norris, D. J.; Bawendi, M. G. Synthesis and characterization of nearly monodisperse CdE (e = sulfur, selenium, tellurium) semiconductor nanocrystallites. *J. Am. Chem. Soc.* **1993**, 115, 8706–8715.
- (11) Talapin, D. V.; Nelson, J. H.; Shevchenko, E. V.; Aloni, S.; Sadtler, B.; Alivisatos, A. P. Seeded growth of highly luminescent CdSe/CdS nanoheterostructures with rod and tetrapod morphologies. *Nano Lett.* **2007**, *7*, 2951–2959.
- (12) Beberwyck, B. J.; Surendranath, Y.; Alivisatos, A. P. Cation exchange: A versatile tool for nanomaterials synthesis. *J. Phys. Chem. C* **2013**, *117*, 19759–19770.
- (13) Gupta, J. A.; Awschalom, D. D.; Efros, A. L.; Rodina, A. V. Spin dynamics in semiconductor nanocrystals. *Phys. Rev. B: Condens. Matter Mater. Phys.* **2002**, *66*, 125307.
- (14) Kim, J.; Wong, C. Y.; Scholes, G. D. Exciton fine structure and spin relaxation in semiconductor colloidal quantum dots. *Acc. Chem. Res.* **2009**, *42*, 1037–1046.
- (15) DiVincenzo, D. P. The physical implementation of quantum computation. *Fortschr. Phys.* **2000**, *48*, 771–783.
- (16) Hu, R.; Yakovlev, D. R.; Liang, P.; Qiang, G.; Chen, C.; Jia, T.; Sun, Z.; Bayer, M.; Feng, D. Origin of two larmor frequencies in the coherent spin dynamics of colloidal CdSe quantum dots revealed by controlled charging. *J. Phys. Chem. Lett.* **2019**, *10*, 3681–3687.
- (17) Siebers, B.; Biadala, L.; Yakovlev, D. R.; Rodina, A. V.; Aubert, T.; Hens, Z.; Bayer, M. Exciton spin dynamics and photo-luminescence polarization of CdSe/CdS dot-in-rod nanocrystals in high magnetic fields. *Phys. Rev. B: Condens. Matter Mater. Phys.* **2015**, *91*, 155304.
- (18) Ma, H.; Jin, Z.; Zhang, Z.; Li, G.; Ma, G. Exciton spin relaxation in colloidal CdSe quantum dots at room temperature. *J. Phys. Chem. A* **2012**, *116*, 2018–2023.
- (19) Huxter, V. M.; Kim, J.; Lo, S. S.; Lee, A.; Nair, P. S.; Scholes, G. D. Spin relaxation in zinc blende and wurtzite CdSe quantum dots. *Chem. Phys. Lett.* **2010**, *491*, 187–192.

- (20) Brovelli, S.; Schaller, R. D.; Crooker, S. A.; García-Santamaría, F.; Chen, Y.; Viswanatha, R.; Hollingsworth, J. A.; Htoon, H.; Klimov, V. I. Nano-engineered electron—hole exchange interaction controls exciton dynamics in core—shell semiconductor nanocrystals. *Nat. Commun.* **2011**, *2*, 280.
- (21) Nirmal, M.; Norris, D. J.; Kuno, M.; Bawendi, M. G.; Efros, A. L.; Rosen, M. Observation of the "dark exciton" in CdSe quantum dots. *Phys. Rev. Lett.* **1995**, *75*, 3728–3731.
- (22) Nelson, J. N.; Zhang, J.; Zhou, J.; Rugg, B. K.; Krzyaniak, M. D.; Wasielewski, M. R. CNOT gate operation on a photogenerated molecular electron spin-qubit pair. *J. Chem. Phys.* **2020**, *152*, 014503.
- (23) Atzori, M.; Sessoli, R. The second quantum revolution: Role and challenges of molecular chemistry. *J. Am. Chem. Soc.* **2019**, *141*, 11339–11352.
- (24) Bloom, B. P.; Graff, B. M.; Ghosh, S.; Beratan, D. N.; Waldeck, D. H. Chirality control of electron transfer in quantum dot assemblies. *J. Am. Chem. Soc.* **2017**, *139*, 9038–9043.
- (25) Bloom, B. P.; Kiran, V.; Varade, V.; Naaman, R.; Waldeck, D. H. Spin selective charge transport through cysteine capped CdSe quantum dots. *Nano Lett.* **2016**, *16*, 4583–4589.
- (26) Mtangi, W.; Kiran, V.; Fontanesi, C.; Naaman, R. Role of the electron spin polarization in water splitting. *J. Phys. Chem. Lett.* **2015**, *6*, 4916–4922.
- (27) Peer, N.; Dujovne, I.; Yochelis, S.; Paltiel, Y. Nanoscale charge separation using chiral molecules. *ACS Photonics* **2015**, *2*, 1476–1481.
- (28) Abendroth, J. M.; Stemer, D. M.; Bloom, B. P.; Roy, P.; Naaman, R.; Waldeck, D. H.; Weiss, P. S.; Mondal, P. C. Spin selectivity in photoinduced charge-transfer mediated by chiral molecules. *ACS Nano* **2019**, *13*, 4928–4946.
- (29) Bender, J. A.; Raulerson, E. K.; Li, X.; Goldzak, T.; Xia, P.; Van Voorhis, T.; Tang, M. L.; Roberts, S. T. Surface states mediate triplet energy transfer in nanocrystal-acene composite systems. *J. Am. Chem. Soc.* 2018, 140, 7543–7553.
- (30) Li, X.; Huang, Z.; Zavala, R.; Tang, M. L. Distance-dependent triplet energy transfer between CdSe nanocrystals and surface bound anthracene. *J. Phys. Chem. Lett.* **2016**, *7*, 1955–1959.
- (31) Mongin, C.; Garakyaraghi, S.; Razgoniaeva, N.; Zamkov, M.; Castellano, F. N. Direct observation of triplet energy transfer from semiconductor nanocrystals. *Science* **2016**, *351*, *369*–372.
- (32) Jin, T.; Uhlikova, N.; Xu, Z.; Zhu, Y.; Huang, Y.; Egap, E.; Lian, T. Enhanced triplet state generation through radical pair intermediates in bodipy-quantum dot complexes. *J. Chem. Phys.* **2019**, *151*, 241101.
- (33) Weinberg, D. J.; Dyar, S. M.; Khademi, Z.; Malicki, M.; Marder, S. R.; Wasielewski, M. R.; Weiss, E. A. Spin-selective charge recombination in complexes of CdS quantum dots and organic hole acceptors. *J. Am. Chem. Soc.* **2014**, *136*, 14513–14518.
- (34) Wang, J.; Ding, T.; Nie, C.; Wang, M.; Zhou, P.; Wu, K. Spin-controlled charge-recombination pathways across the inorganic/organic interface. *J. Am. Chem. Soc.* **2020**, *142*, 4723–4731.
- (35) Hore, P. J. The triplet mechanism of chemically induced dynamic electron polarization. A vector model. *Chem. Phys. Lett.* **1980**, *69*, 563–566.
- (36) Hore, P. J.; Joslin, C. G.; McLauchlan, K. A. The role of chemically-induced dynamic electron polarization (CIDEP) in chemistry. *Chem. Soc. Rev.* **1979**, *8*, 29–61.
- (37) Steiner, U. E.; Ulrich, T. Magnetic field effects in chemical kinetics and related phenomena. *Chem. Rev.* **1989**, 89, 51–147.
- (38) Wong, S. K.; Hutchinson, D. A.; Wan, J. K. S. Chemically induced dynamic electron polarization. II. General theory for radicals produced by photochemical reactions of excited triplet carbonyl compounds. *J. Chem. Phys.* **1973**, *58*, 985–9.
- (39) Kobori, Y.; Fuki, M.; Murai, H. Electron spin polarization transfer to the charge-separated state from locally excited triplet configuration: Theory and its application to characterization of geometry and electronic coupling in the electron donor-acceptor system. *J. Phys. Chem. B* **2010**, *114*, 14621–14630.
- (40) Olshansky, J. H.; Ding, T. X.; Lee, Y. V.; Leone, S. R.; Alivisatos, A. P. Hole transfer from photoexcited quantum dots: The

- relationship between driving force and rate. J. Am. Chem. Soc. 2015, 137, 15567–15575.
- (41) Boehme, S. C.; Wang, H.; Siebbeles, L. D. A.; Vanmaekelbergh, D.; Houtepen, A. J. Electrochemical charging of CdSe quantum dot films: Dependence on void size and counterion proximity. *ACS Nano* **2013**, *7*, 2500–2508.
- (42) Gosztola, D.; Niemczyk, M. P.; Svec, W.; Lukas, A. S.; Wasielewski, M. R. Excited doublet states of electrochemically generated aromatic imide and diimide radical anions. *J. Phys. Chem. A* **2000**, *104*, 6545–6551.
- (43) Chen, O.; Zhao, J.; Chauhan, V. P.; Cui, J.; Wong, C.; Harris, D. K.; Wei, H.; Han, H.-S.; Fukumura, D.; Jain, R. K.; Bawendi, M. G. Compact high-quality CdSe-CdS core-shell nanocrystals with narrow emission linewidths and suppressed blinking. *Nat. Mater.* **2013**, *12*, 445–451.
- (44) Gomes, R.; Hassinen, A.; Szczygiel, A.; Zhao, Q.; Vantomme, A.; Martins, J. C.; Hens, Z. Binding of phosphonic acids to CdSe quantum dots: A solution NMR study. *J. Phys. Chem. Lett.* **2011**, *2*, 145–152.
- (45) Zhu, H.; Song, N.; Lian, T. Wave function engineering for ultrafast charge separation and slow charge recombination in type II core/shell quantum dots. *J. Am. Chem. Soc.* **2011**, *133*, 8762–8771.
- (46) Zhu, H.; Song, N.; Rodriguez-Cordoba, W.; Lian, T. Wave function engineering for efficient extraction of up to nineteen electrons from one CdSe/CdS quasi-type II quantum dot. *J. Am. Chem. Soc.* **2012**, *134*, 4250–4257.
- (47) Bodunov, E. N.; Antonov, Y. A.; Gamboa, A. L. S. On the origin of stretched exponential (kohlrausch) relaxation kinetics in the room temperature luminescence decay of colloidal quantum dots. *J. Chem. Phys.* **2017**, *146*, 114102.
- (48) Zhu, H.; Song, N.; Lian, T. Controlling charge separation and recombination rates in CdSe/ZnS type I core-shell quantum dots by shell thicknesses. *J. Am. Chem. Soc.* **2010**, *132*, 15038–15045.
- (49) Dworak, L.; Matylitsky, V. V.; Breus, V. V.; Braun, M.; Basche, T.; Wachtveitl, J. Ultrafast charge separation at the CdSe/CdS core/shell quantum dot/methylviologen interface: Implications for nanocrystal solar cells. *J. Phys. Chem. C* **2011**, *115*, 3949–3955.
- (50) Zeng, P.; Kirkwood, N.; Mulvaney, P.; Boldt, K.; Smith, T. A. Shell effects on hole-coupled electron transfer dynamics from CdSe/CdS quantum dots to methyl viologen. *Nanoscale* **2016**, *8*, 10380–10387.
- (51) de Sousa, J. S.; Freire, J. A. K.; Farias, G. A. Exciton escape in CdSe core-shell quantum dots: Implications for the development of nanocrystal solar cells. *Phys. Rev. B: Condens. Matter Mater. Phys.* **2007**, *76*, 155317.
- (52) Olshansky, J. H.; Balan, A. D.; Ding, T. X.; Fu, X.; Lee, Y. V.; Alivisatos, A. P. Temperature-dependent hole transfer from photoexcited quantum dots to molecular species: Evidence for trapmediated transfer. *ACS Nano* **2017**, *11*, 8346–8355.
- (53) Rinehart, J. D.; Schimpf, A. M.; Weaver, A. L.; Cohn, A. W.; Gamelin, D. R. Photochemical electronic doping of colloidal CdSe nanocrystals. *J. Am. Chem. Soc.* **2013**, *135*, 18782–18785.
- (54) Whitaker, K. M.; Ochsenbein, S. T.; Polinger, V. Z.; Gamelin, D. R. Electron confinement effects in the EPR spectra of colloidal n-type ZnO quantum dots. *J. Phys. Chem. C* **2008**, *112*, 14331–14335.
- (55) Dubinski, A. A.; Perekhodtsev, G. D.; Poluektov, O. G.; Rajh, T.; Thurnauer, M. C. Analytical treatment of EPR spectra of weakly coupled spin-correlated radical pairs in disordered solids: Application to the charge-separated state in TiO<sub>2</sub> nanoparticles. *J. Phys. Chem. B* **2002**, *106*, 938–944.
- (56) Rajh, T.; Poluektov, O.; Dubinski, A. A.; Wiederrecht, G.; Thurnauer, M. C.; Trifunac, A. D. Spin polarization mechanisms in early stages of photoinduced charge separation in surface-modified TiO<sub>2</sub> nanoparticles. *Chem. Phys. Lett.* **2001**, *344*, 31–39.
- (57) Carmieli, R.; Thazhathveetil, A. K.; Lewis, F. D.; Wasielewski, M. R. Photoselective DNA hairpin spin switches. *J. Am. Chem. Soc.* **2013**, *135*, 10970–10973.
- (58) Michaeli, S.; Meiklyar, V.; Endeward, B.; Mobius, K.; Levanon, H. Photoinduced electron transfer between C<sub>60</sub> and N,N,N',N'-

tetramethylbenzidine (NTMB). Fourier transform electron paramagnetic resonance study. *Res. Chem. Intermed.* **1997**, 23, 505–517. (59) Garcia-Santamaria, F.; Chen, Y.; Vela, J.; Schaller, R. D.; Hollingsworth, J. A.; Klimov, V. I. Suppressed auger recombination in "giant" nanocrystals boosts optical gain performance. *Nano Lett.* **2009**, *9*, 3482–3488.